Outskirts of Galaxy Clusters: Intense Life in the Suburbs
Proceedings IAU Colloquium No. 195, 2004
A. Diaferio, ed.

DOI: 10.1017/S1743921304000407

Optical and X-ray analysis of the galaxy cluster A3921

C. Ferrari[1,2]†, C. Benoist[2], S. Maurogordato[2], A. Cappi[3], E. Slezak[2], E. Belsole[4,5]‡, J. L. Sauvageot[4], H. Bourdin[2] and G. W. Pratt[4,6] ¶

[1] Institut für Astrophysik, Universität Innsbruck, Technikerstraße 25, A-6020 Innsbruck, Austria

[2] CERGA, UMR 6527, CNRS, Observatoire de la Cte d'Azur, BP 4229, Le Mont-Gros, 06304 Nice Cedex 4, France

[3] INAF, Osservatorio Astronomico di Bologna, via Ranzani 1, I-40127 Bologna, Italy

[4] Service d'Astrophysique, CEA Saclay, L'Orme des Merisiers Bât 709, F-91191 Gif-sur-Yvette, France

[5] H.H. Wills Physics Laboratory, University of Bristol, Tyndall Avenue, Bristol BS8 1TL, U.K.

[6] Max-Planck-Institut für extraterrestrische Physik, Postfach 1312, 85741 Garching, Germany

Abstract. We present the analysis and results of a new spectroscopic and photometric survey of the central 1.5 Mpc^2 region of the galaxy cluster A3921 (z=0.094). We detect the presence of two dominant clumps of galaxies with a mass ratio of ∼4-5: a main cluster centered on the BCG (A3921-A), and a NW sub-cluster (A3921-B) hosting the second brightest cluster object. By comparing optical results to the X-ray analysis of XMM observations (Belsole *et al.* 2004), we find that A3921-B is tangentially traversing the main cluster along a SW/NE direction. The analysis of stellar populations of more than one hundred cluster members reveals that the merger event has probably affected the kinematics and spectral properties of the active galaxies in A3921.

1. Introduction

In the standard cosmological scenario of hierarchical structure formation, galaxy clusters form by the merger of less massive systems. Combined optical and X-ray studies have been particularly successful in revealing the complex dynamics of merging clusters (e.g. Davis *et al.* 1995, Durret *et al.* 1998, Arnaud *et al.* 2000). This field is more and more active since precise spectro-imaging data in X-rays is now available with Chandra and XMM, allowing us to derive spatially resolved temperature and density maps, in which very typical signatures of merging have been detected.

In this paper we present the analysis of new spectroscopic and imaging data relative to the cluster A3921 with EFOSC2 and WFI at the ESO 3.6 and 2.2 m telescopes respectively (Ferrari *et al.* 2004). These optical results are compared with the new XMM-Newton X-ray analysis of the cluster (Belsole *et al.* 2004).

† This research was supported in part by Marie Curie individual fellowships MEIF-CT-2003-900773.

‡ This research was supported in part by PPARC.

¶ This research was supported in part by Marie Curie individual fellowship MEIF-CT-2003-500915.

2. Optical morphology

In the top panel of Fig. 1, the iso-density contours of the projected distribution of galaxies belonging to the red-sequence of A3921 up to R=18.2 (corresponding to R=R*+2) are overlaid on the R-band image of the central field of the cluster. A3921 is clearly characterized by a bimodal morphology, with two main sub-clusters (hereafter A and B), as confirmed by the application of a classical segmentation algorithm to the iso-density map of A3921. Using a threshold of 3 times the r.m.s of the map, this algorithm detect two domains. For each of them, the position of the pixel with the highest density and the two first barycentric moments are estimated, allowing us to define the center and the orientation (*i.e.* the position angle) of each clump. A visual inspection of the optical iso-density contours reveals that the double morphology of A3921 is quite distorted. In particular, the clump A3921-B is characterized by a twisting of the iso-density contours from the internal to the external regions of the sub-cluster, and by the presence of a less dense Southern tail. This analysis is quantitatively confirmed by applying our segmentation algorithm with a threshold of 4 times the r.m.s of the map. In this case (dashed lines in the top panel of Fig. 1), the general elongation of the clump B varies significantly from the 3σ clipping case. A3921-B is more elongated towards the South for the fainter density cut, following the Southern tail of the clump and confirming a twisting of the optical iso-density contours. The shape of A3921-A is much more regular, but in both cases an offset of the optical density maxima from the two BCGs' positions is observed.

3. Pre- or post-merger?

The optical morphology of A3921 suggests that this cluster consists of two interacting systems. Therefore, in the following we will try to understand if they are in a pre- or post-merger phase.

3.1. *Dynamical analysis*

Both the velocity distribution of the whole cluster and those of the two clumps separately do not show any evidence for merging, as they are not significantly different from a Gaussian distribution. Moreover, we observe a very small difference in the mean velocities of the two sub-clusters (Δv$\simeq$90 km/s, well within the velocity dispersion of each individual subcluster). Using the estimate of the velocity dispersion of each sub-cluster, we have calculated the virial masses of A3921-A and B inside the two circles of the top panel of Fig. 1 (R$\simeq$0.4 Mpc), obtaining a quite high mass ratio between these two components ($\sim$4-5).

The analysis of the velocity distribution, however, does not answer our main question about the dynamical state of the cluster. We have thus applied the two-body dynamical formalism to the sub-structures of A3921. Because parametric solutions to the equations of motion can be derived both in the bound and unbound case, this method allows us to determine the dynamical state of the cluster by studying the solutions of the equation of motions as a function of α, *i.e.* the angle between the line connecting the two systems and the plane of the sky (Beers *et al.* 1982). We have made several tests under the hypothesis that a) the two sub-clusters have never collided before, or have collided b) 0.25, c) 0.50 and d) 1.00 Gyr ago. The results of these tests are summarized in Tab. 1.

3.2. *Comparison with X-ray results and discussion*

From Tab. 1 we can see that several solutions could explain the observed dynamics of A3921. A comparison with the X-ray properties of the cluster can allow us to understand which of them we can accept.

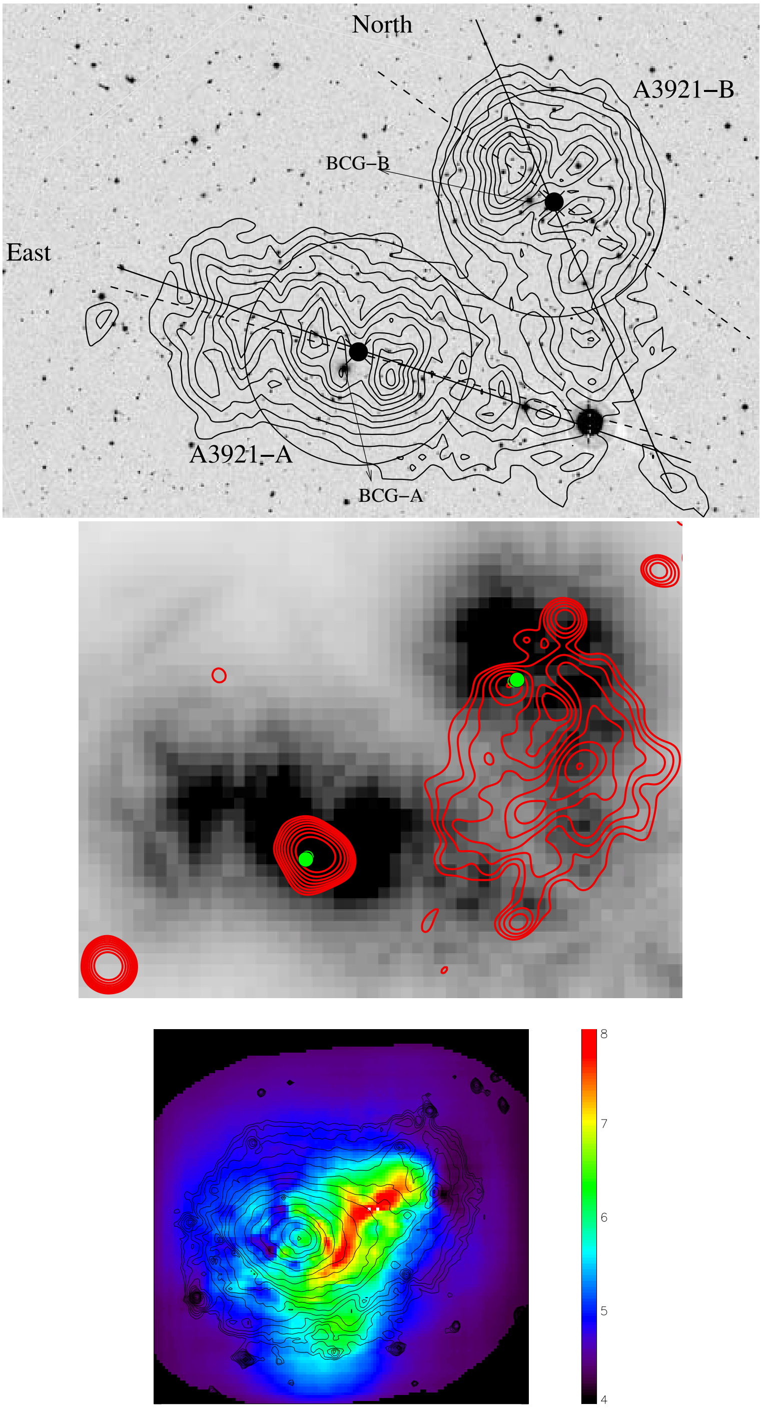

Figure 1. Top: Optical iso-density contours overlaid on the R–band image of A3921 central field (30×20 arcmin^2). The lines (solid and dashed) and the black small circles show respectively the orientation and the centre of the two subclusters (see text). The dynamical analysis of each clump has been done on the galaxies inside the two black circles (R$\simeq$ 0.4 Mpc). The positions of the brightest galaxies of the two sub-clusters are also shown – **Middle:** X-ray residuals above a 2D-β model overlaid on the red sequence galaxy iso-density map up to R=R*+2. The positions of the brightest galaxies of the two sub-clusters are indicated by small circles – **Bottom :** Temperature map of A3921 obtained by applying the wavelet algorithm described in Bourdin *et al.* 2004.

https://doi.org/10.1017/S1743921304000407 Published online by Cambridge University Press

Scenario	T_0 [Gyr]	V [km/s]	R [Mpc]	α [deg]	Solutions
a1	12.60	90.43	7.31	84.19	outgoing
a2	"	90.01	6.04	82.97	incoming
a3	"	2211	0.741	3.822	incoming
b	0.25	1582	0.741	3.29	outgoing
c	0.50	198	0.83	26.99	outgoing
d1	1.00	73.45	1.28	54.67	outgoing
d2	"	116.6	1.166	50.60	incoming
d3	"	1069.3	0.7424	4.175	incoming

Table 1. Possible solutions for the two-body dynamical model. Col.1: ID of the possible scenario – Col.2: time since last interaction between the two clumps – Col.3: relative velocity between the two clumps – Col.4: spatial separation between the two systems – Col.5: angle between the plane of the sky and the line connecting the centers of the two clumps – Col.6: state of the systems for the possible solutions

The analysis of XMM-Newton observations by Belsole *et al.* 2004 reveals that A3921 is characterized by a bimodal morphology in the X-ray domain too. The X-ray emission of A3921-A can be modelled with a 2Dβ-model, leaving a distorted residual structure toward the NW, coincident with A3921-B (middle panel of Fig. 1). The main cluster detected in X-ray is centered on the BCG position, while the X-ray peak of the NW clump is offset from the brightest galaxy of A3921-B. The temperature map of the cluster shows an extended hot region oriented parallel to the line joining the centres of the two sub-clusters (bottom panel of Fig. 1). A comparison of this image with numerical simulations by Ricker & Sarazin (2001) suggests that we are observing the central phases of an off axis merger between two unequal mass objects, where clump A is the most massive component, consistent with optical results.

By combining the signatures of merging derived both from the optical iso-density map and from X-ray results, we can now reconsider the solutions of the two-body dynamical model (Tab. 1). The high angle solutions of cases a1) and a2) would imply a very large real separation for the two sub-clusters, which is very unlikely taking into account the clear signs of interaction between the two clumps. We can also exclude the c) solution, as we expect a higher value of the relative velocity ($\geqslant$1000 km/s) between the two clumps for obtaining a so evident hot bar in the temperature map. Finally, the comparison of the observed and simulated temperature maps clearly exclude an older merger (e.g. t_0=1 Gyr ago), as we should not detect such obvious structure in the temperature map. Therefore, only the solutions corresponding to the very central phases of merging seem to be possible to explain all our observational results, implying a collision axis nearly perpendicular to the line of sight consistent with the observed velocity distribution.

The superimposition of the X-ray residuals on the optical iso-density map (middle panel of Fig. 1) shows that the bulk of X-ray emission in A3921-B is offset towards SW from the main concentration of galaxies. As numerical simulations show that the non-collisional component is much less affected by the collision than the gas distribution, this offset suggests that A3921-B is tangentially traversing A3921-A along a SW/NE direction, with its galaxies in advance with respect to the gaseous component. This off-axis collision scenario is consistent with the shape of the feature in the temperature map (Belsole *et al.* 2004). From a comparison of the galaxy density maps to those obtained in numerical simulations with different impact parameters before and after the collision, the orientation of the NW group tail also suggests that it has already tangentially crossed the main cluster (Ferrari *et al.* 2004). As the structure of the group seems preserved,

https://doi.org/10.1017/S1743921304000407 Published online by Cambridge University Press

the collision has probably occured on the edge of the cluster, confirming the results from the X-ray analysis.

4. Star-formation properties of A3921 galaxies

We have analysed the effects of the merging event on star formation in A3921 galaxies. Following the classification scheme by Dressler *et al.* (1999), we have divided the cluster members into passive (k-type), post-starburst (k+a and a+k types) and emission-line galaxies (e type). 76% of A3921 galaxies belong to the first group, while the remaining 24% show evidence of recent or ongoing star formation. In particular we find a high percentage of emission line galaxies with respect to similar studies on other low redshift clusters (e.g. Barrena *et al.* 2002). These objects seem to be localized in the region surrounding the hotter temperature bar detected in the X-ray. Even if a wider spectroscopic coverage is necessary to assess the presence of such a spatial correlation, a 2D Kolmogorov-Smirnov test rejects the hypothesis that the positions of k and e-types galaxies are drawn from the same parent population with an extremely low significance level (∼0.1%). Moreover, by analysing separately the velocity distributions of passive and active galaxies, we find that a) active objects are characterized by a significantly higher velocity dispersion and a non-Gaussian velocity distribution, and b) a K-S test rejects the hypothesis that the two velocity datasets are drawn from the same parent population with a significance level of ∼8%. It is therefore possible that both the kinematics and spectral properties of the active galaxies in A3921 have been influenced by the merging event.

References

Arnaud, M., Maurogordato, S., Slezak, E., & Rho, J., 2000, A&A, 355, 461
Barrena, R., Biviano, A., Ramella, M., Falco, E.E., & Seitz, S., 2002, A&A, 386, 861B
Beers, T.C., Geller, M.J.& Huchra, J.P., 1982, ApJ, 257, 23
Belsole, E. et al., 2004, in preparation
Bourdin, H., Sauvageot, J.L., Slezak, E., Bijaoui, A., & Teyssier, R., 2004, A&A, 414, 429
Davis, D.S., Bird, C.M., Mushotzky, R.F., & Odewahn, S.C., 1995, ApJ, 440, 48
Dressler, A., Smail, I., Poggianti, B.M., Butcher, H., Couch, W.J., Ellis, R.S., & Oemler, A., 1999, ApJ, 122, 51
Durret, F., Forman, W., Gerbal, D., Jones, C., & Vikhlinin, A., 1998, A&A, 335, 41
Ferrari, C. et al., 2004, in preparation
Ricker, P.M., & Sarazin, C.L., 2001, ApJ, 561, 621